NASA TN D-903

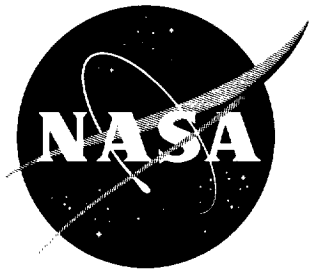

TECHNICAL NOTE

D-903

EFFECT AT HIGH SUBSONIC SPEEDS OF FUSELAGE FOREBODY STRAKES ON THE STATIC STABILITY AND VERTICAL-TAIL-LOAD CHARACTERISTICS OF A COMPLETE MODEL HAVING A DELTA WING

By Edward C. Polhamus and Kenneth P. Spreemann

Langley Research Center
Langley Field, Va.

NATIONAL AERONAUTICS AND SPACE ADMINISTRATION
WASHINGTON

May 1961

NATIONAL AERONAUTICS AND SPACE ADMINISTRATION

TECHNICAL NOTE D-903

EFFECT AT HIGH SUBSONIC SPEEDS OF FUSELAGE FOREBODY STRAKES ON THE STATIC STABILITY AND VERTICAL-TAIL-LOAD CHARACTERISTICS OF A COMPLETE MODEL HAVING A DELTA WING[1]

By Edward C. Polhamus and Kenneth P. Spreemann

SUMMARY

A wind-tunnel investigation at high subsonic speeds has been conducted to determine the effect of fuselage forebody strakes on the static stability and the vertical-tail-load characteristics of an airplane-type configuration having a delta wing. The tests were made at Mach numbers from 0.60 to 0.92 corresponding to Reynolds numbers from 3.0×10^6 to 4.2×10^6, based on the wing mean aerodynamic chord, and at angles of attack from approximately -2° to 24°. The strakes provided improvements in the directional stability characteristics of the wing-fuselage configuration which were reflected in the characteristics of the complete configuration in the angle-of-attack range where extreme losses in directional stability quite often occur. It was also found that the strakes, through their beneficial effect on the wing-fuselage directional stability, reduced the vertical-tail load per unit restoring moment at high angles of attack. The results also indicated that, despite the inherent tendency for strakes to produce a pitch-up, acceptable pitching-moment characteristics can be obtained provided the strakes are properly chosen and used in conjunction with a wing-body-tail configuration characterized by increasing stability with increasing lift.

INTRODUCTION

The trend of aircraft configurations toward low aspect ratio or relatively highly swept wings, in order to provide the desired performance, has made it necessary for these configurations quite often to operate at rather high angles of attack. In addition, the trend toward

[1]Supersedes the recently declassified NACA Research Memorandum L57K15a, by Edward C. Polhamus and Kenneth P. Spreemann, 1958.

high fuselage mass loadings and long noses have made these configurations susceptible to rather violent motions (see refs. 1 to 3) in which extremely high angles of attack can be encountered. These trends, therefore, have made the variation of directional stability with angle of attack very important and, unfortunately, large deficiencies in static directional stability are often encountered at high angles of attack. Although a portion of this deficiency is associated with losses in vertical-tail effectiveness, the increase in wing-fuselage instability with increasing angle of attack (which is characteristic of rather a large number of conventional configurations see ref. 4)) plays an important role. It has been shown in reference 5 that these wing-fuselage characteristics usually are associated with the flow field induced on the fuselage afterbody by the wing and that the directional stability (relative to the body axis) is essentially independent of angle of attack when the afterbody is removed. In reference 6 it is shown that placing the afterbody volume in two bodies outboard on the wing (forming a three-body configuration) results in a wing-fuselage configuration that has a desirable reduction in directional instability with angle of attack and even becomes stable at high angles of attack. Although this type of configuration appears promising from several standpoints, less extreme configuration changes are also of interest, and reference 7 describes a relatively simple modification which results in desirable directional stability characteristics. This modification consists of a narrow strake (or flange) placed on the fuselage forebody in the horizontal plane and running from the nose to the wing leading edge. This modification improved the directional stability at high angles of attack through its effect on the wing-fuselage configuration which actually became stable at high angles of attack with the strake on. For the particular configuration of reference 7, however, improvements in directional stability were accompanied by pitch-up tendencies due to the nonlinear lift characteristics of these strakes.

The purpose of the present investigation, therefore, is to study the application of strakes to a configuration for which increased linearity of longitudinal characteristics might be expected while at the same time the directional stability is improved. For this reason a configuration having a basic 45° delta wing clipped to aspect ratio 3 and a low horizontal tail was selected, since results of reference 8 indicate that this configuration has the type of longitudinal stability characteristics (stability increasing with angle of attack) that might be made more linear by use of strakes. In addition to the stability characteristics, the effect of strakes on the loads carried by the exposed vertical tail will also be presented.

COEFFICIENTS AND SYMBOLS

Figure 1 shows the body system of axes used in data reduction with arrows indicating positive direction of forces, moments, and angles. The coefficients and symbols used are defined as follows:

C_L lift coefficient, $\frac{\text{Lift}}{qS}$

C_D drag coefficient, $\frac{\text{Drag}}{qS}$

C_m pitching-moment coefficient, $\frac{\text{Pitching moment}}{qS\bar{c}}$

C_l rolling-moment coefficient, $\frac{\text{Rolling moment}}{qSb}$

C_n yawing-moment coefficient, $\frac{\text{Yawing moment}}{qSb}$

C_Y side-force coefficient, $\frac{\text{Side force}}{qS}$

$C_{B,V}$ vertical-tail root-bending-moment coefficient, $\frac{\text{Vertical-tail root-bending moment}}{qS_V b_V}$

$C_{n,V}$ vertical-tail yawing-moment coefficient, $\frac{\text{Vertical-tail yawing moment}}{qS_V \bar{c}_V}$ (referenced to $\bar{c}_V/4$)

$C_{N,V}$ vertical-tail normal-force coefficient, $\frac{\text{Vertical-tail normal force}}{qS_V}$

l fuselage length

q dynamic pressure, $\frac{\rho V^2}{2}$, lb/sq ft

ρ mass density of air, slugs/cu ft

V free-stream velocity, ft/sec

M Mach number

S wing area, 2.20 sq ft

S_V exposed vertical-tail area, 0.435 sq ft

c local wing chord parallel to plane of symmetry

$\bar{c}$ wing mean aerodynamic chord, $\frac{2}{S}\int_0^{b/2} c^2 dy$, ft

$\bar{c}_h$ mean aerodynamic chord of horizontal tail, ft

$\bar{c}_V$ vertical-tail mean aerodynamic chord, ft

b wing span, ft

b_V exposed vertical-tail span, 0.661 ft

y spanwise distance from plane of model symmetry, ft

α angle of attack, deg

β angle of sideslip, deg

$$C_{l_\beta} = \frac{\partial C_l}{\partial \beta}$$

$$C_{n_\beta} = \frac{\partial C_n}{\partial \beta}$$

$$C_{Y_\beta} = \frac{\partial C_Y}{\partial \beta}$$

$$\left(C_{B_\beta}\right)_V = \frac{\partial C_{B,V}}{\partial \beta}$$

$$\left(C_{n_\beta}\right)_V = \frac{\partial C_{n,V}}{\partial \beta}$$

$$\left(C_{N_\beta}\right)_V = \frac{\partial C_{N,V}}{\partial \beta}$$

Subscripts:

w	wing
f	fuselage

MODEL AND APPARATUS

A two-view drawing of the complete model showing the general arrangement and some of the pertinent dimensions is given in figure 2. Details of the fuselage are presented in figure 3, while those of the various forebody strakes are presented in figure 4. The wing, which was mounted on the fuselage in the midposition, was constructed of aluminum and had an aspect ratio of 3, taper ratio of 0.14, leading-edge sweep of 45°, and an NACA 65A006 airfoil section parallel to the plane of symmetry. The horizontal tail was constructed of steel covered with plastic and fiber glass, had a triangular plan form of aspect ratio 4, and an NACA 65A006 airfoil section parallel to the plane of symmetry. The vertical tail, which was also constructed of steel covered with plastic and fiber glass, had an aspect ratio and taper ratio (based on the effective exposed plan form indicated in fig. 2) of 1.02 and 0.46, respectively, a quarter-chord sweep angle of 28°, and an NACA 65A006 airfoil section parallel to the plane of symmetry. The fuselage (see fig. 3) was constructed of aluminum, had a fineness ratio of 10.94, and consisted of an ogival nose, a cylindrical center section, and a boattailed afterbody. The fuselage forebody strakes were constructed of 0.05-inch brass and the three lengths and two widths indicated in figure 4 were investigated.

The model was tested on the sting-type support system shown in figure 5. With this support system the model can be remotely operated through approximately 26° angle range in the plane of the vertical strut. The model can be rotated 90° so that either angle of attack or angle of sideslip can be the remotely controlled variable. With the wings horizontal, couplings can be used to support the model at angles of sideslip of -4° and 4°, while the model is tested through the angle-of-attack range.

The forces and moments acting on the model were measured by means of a six-component electrical strain-gage balance mounted internally in the fuselage, while a three-component electrical strain-gage balance (mounted internally in the fuselage at the base of the vertical tail) measured the forces and moments acting on the vertical tail. In order to minimize air leakage through the small gap which existed between the

fuselage and the vertical tail at their juncture, a sponge-rubber seal was utilized. Some details of the system used to measure the vertical-tail loads are presented in figure 6.

TESTS

The sting-supported model was tested in the Langley high-speed 7- by 10-foot tunnel through a Mach number range of 0.60 to 0.92, which corresponds to a Reynolds number range from about 3.0×10^6 to 4.2×10^6, based on the wing mean aerodynamic chord. The longitudinal characteristics were obtained at zero sideslip through an angle-of-attack range which, at a Mach number of 0.60, varied from approximately -2° to 24°. At the higher Mach numbers the complete angle-of-attack range was not obtained due to tunnel power limitations. The effect of angle of attack on the lateral- and directional-stability derivatives and the vertical-tail-load derivatives was obtained by testing the model at angles of sideslip of $\pm 4^\circ$ (by the use of bent couplings inserted in the sting system) through the angle-of-attack range. This technique of obtaining derivatives requires, of course, the assumption that the forces and moments vary linearly with sideslip angle. In order to determine the degree of linearity and effects of higher sideslip angles, a limited number of tests were obtained by rotating the model 90° and testing through a range of sideslip angles at a constant angle of attack.

CORRECTIONS

Jet-boundary corrections to the angle of attack were applied in accordance with reference 9. The corrections to the pitching moment, lateral force, yawing moment, and rolling moment were negligible and therefore were not applied. Past experience has indicated that tare values should be very small, and, therefore, no tares were applied. Blockage corrections were applied to the data by the method outlined in reference 10.

The angle of attack and angle of sideslip have been corrected for deflection of the sting support and balance system under load. No attempt has been made to correct the data for aeroelastic distortion of the model. In order to provide sufficient instrumentation for the tail-load measurements, the fuselage base-pressure measurements were omitted and, therefore, the drag results have not been corrected to the condition of free-stream pressure at the fuselage base.

RESULTS AND DISCUSSION

Presentation of Results

The basic longitudinal data and the lateral stability parameters (based on ±4° sideslip) are presented in figures 7 and 8 for several Mach numbers and configurations. Figures 9 and 10 present the effect of strakes on the variation of the aerodynamic characteristics with sideslip angle, whereas figures 11 and 12 present the variation of the vertical-tail-load characteristics with angle of attack for several Mach numbers and configurations. It will be noted throughout the figures that complete data for all of the strakes shown in figure 4 are not presented. Since the main purpose of this investigation was to determine the directional stability and vertical-tail-load characteristics for a strake configuration which had acceptable longitudinal stability characteristics, it was decided to minimize the tunnel testing time by determining the longitudinal stability characteristics for the complete model with each of the strakes at a Mach number of 0.60 and to limit all other tests to the most promising strakes.

Longitudinal Stability

The effect of the fuselage forebody strakes on the longitudinal characteristics are presented in figure 7 for various model configurations. Figure 7(a) presents the lift coefficient as a function of angle of attack for the fuselage alone, the wing-fuselage combination, and the complete-model configuration. In general, the addition of fuselage forebody strakes had small effects throughout the angle-of-attack range except for the largest strake at the higher angles. However, due to the rather large moment arms involved, quite sizeable effects on pitching-moment characteristics are indicated (see fig. 7(b)). As mentioned previously, the complete range of strake sizes were investigated only for the complete-model configuration at a Mach number of 0.60. From these results it will be noted that the largest strake produced an extremely undesirable "pitch-up" at the relatively low angle of attack of 8°. This is apparently associated, for the most part, with the nonlinear lift variation which characterizes low-aspect-ratio lifting surfaces and which is accentuated by the nonlinear variation of body-induced upwash. In an attempt to alleviate this situation, several reductions in strake size were investigated and from the results the 14.38- by 0.50-inch and the 14.38- by 0.25-inch strakes were selected for further study. The effect of these two strakes on the characteristics of the complete-model configuration were studied at Mach numbers up to 0.92. Although there still is considerable pitching-moment nonlinearity, which on an actual aircraft configuration might require some tailoring with regard to "wing fixes" and

horizontal-tail geometry and location, it is felt that the 14.38- by 0.50-inch and 14.38- by 0.25-inch strakes cover fairly well the range of sizes which for this configuration provide reasonable longitudinal stability characteristics and therefore warrant study of their effects on the directional stability and vertical-tail-load characteristics.

Because of the angle-of-attack limitations at the higher Mach numbers, these strakes were selected from the low Mach number results and although the indications are that the strake effects are relatively independent of Mach number it would be desirable to make further studies. It should also be kept in mind that these results were obtained at relatively low Reynolds numbers and that there may be some scale effect.

In order to provide information on possible wing interference effects and downwash changes the 14.38- by 0.50-inch strake was also tested on the fuselage alone and on the wing-fuselage combination, and the results are included in figure 7. As mentioned previously, the fuselage base pressure was not measured and, therefore, it was not possible to correct the drag to the condition of free-stream static pressure at the base. It is felt, however, that the relative effects of the strakes on the drag are valid and therefore the drag results for the complete configuration are presented in figure 7(c). The results indicate that the strakes had a negligible effect on the drag below lift coefficients of about 0.7 and that above this lift coefficient they usually decreased the drag for a given lift coefficient. This result is substantiated in reference 7, where the drag has been corrected for base pressure.

Lateral Stability

The effects of the fuselage forebody strakes on the lateral stability characteristics (obtained from tests at sideslip angles of $\pm 4^{\circ}$) of the fuselage, the wing-fuselage configuration, and the complete configuration are presented in figure 8 as a function of angle of attack. The following discussion will be based on the results obtained at $M = 0.60$ and 0.80 since the angle-of-attack range is largest for these Mach numbers. For the fuselage-alone configuration, the results indicate an extremely large effect of the strakes on the directional stability parameter, C_{n_β}, above an angle of attack of about 13°, with the fuselage becoming neutrally stable at about 18° and exhibiting a rather large degree of positive directional stability at the highest angles of attack tested. With the wing on, the favorable effect of the strakes on directional stability is manifested at a somewhat lower angle of attack, due possibly to the wing induced upwash. However, at the higher angles of attack the effect of the strake is considerably less with the wing on than with the wing off. Inasmuch as the strakes appear to have a rather pronounced effect

on the span load distribution of the wing, as indicated by the change in the effective dihedral parameter C_{l_β}, the reduction in strake contribution to directional stability may be associated with wing interference on the fuselage afterbody. (See ref. 5.) On the right-hand portion of figure 8 the effect of the strakes on the complete-model characteristics is shown, and it will be noted that in general the expected adverse effect of the strake on the vertical tail is relatively small and the overall results reflect the favorable effect on the wing-body configuration. It will be noted that the strakes have rather large effects on the parameters C_{l_β} and C_{Y_β}, and these effects must be considered when predicting the flying qualities of a configuration.

In order to gain some insight as to the range of sideslip angles for which the directional stability parameter reflects the directional stability characteristics, results over a sideslip range are presented for an angle of attack of 15° in figure 9. The results indicate no serious nonlinearities for angles of sideslip less than about 11°.

In order to determine the contribution of each strake, tests on the fuselage alone were run with one strake removed and the results are presented in figure 10 where they are compared with the results obtained with both strakes and with no strakes. The results with one strake indicate a rather large yawing moment and side force at zero sideslip. At zero sideslip the relationship between the side force and yawing moment indicates that the force is probably concentrated in the region of the strake and the direction of the force indicates a lower pressure on the side opposite that containing the strake. It therefore appears that at zero sideslip the strake is acting as a spoiler. The values at zero sideslip are, of course, eliminated when the other strake is added and, with mutual interference neglected, it is the variation of yawing moment with sideslip for each strake which determines the effect of the strakes on the stability. In the moderate sideslip range ($\pm 5^\circ$), it appears that the strake on the windward side has the greater effect since its slope has the greater deviation from the "no strake" slope. As the model is sideslipped to higher angles the forces no longer appear to be concentrated in the region of the strake and the effects appear to be more complicated. For example, at an angle of sideslip of 12° with the strake on the windward side the strake has negligible effect on the yawing moment but contributes a rather large positive increment to the side force. It therefore appears that, in the sideslipped condition at least, the strake has considerable effect on other portions of the fuselage and fuselage pressure-distribution measurements would be desirable in tracing these effects.

Vertical-Tail Loads

The normal-force, yawing-moment, and bending-moment characteristics due to sideslip as measured on the exposed panel of the vertical tail are presented in figure 11 as a function of angle of attack for several Mach numbers. As would be expected from the measured tail contribution to directional stability (see fig. 8) the vertical-tail normal-force coefficient per unit sideslip angle $\left(C_{N_\beta}\right)_V$ decreases rather rapidly at the higher angles of attack. This decrease is associated to a large extent with the sidewash induced at the tail by the fuselage forebody separation vortices and is discussed in some detail in reference 11. Above an angle of attack of about 18° it can be seen that the addition of the fuselage forebody strakes reduced the vertical-tail normal force. A reduction in vertical-tail load per unit sideslip for a configuration which is directionally unstable with the vertical tail off does not imply that the tail loads encountered will be less. In fact the tail load encountered is usually greater for such a configuration since the larger sideslip angle required to produce a restoring moment sufficient to counteract a given displacement results in an increase in the usually unstable wing-fuselage yawing moment which must also be overcome by the vertical tail. A decrease in the unstable wing-fuselage yawing moment will, for a constant value of tail load per unit sideslip, result in a decrease in the tail load per unit restoring moment $\frac{C_{N,V}}{C_n}$. In addition, for a stable wing-fuselage combination, a reduction in the tail load per unit sideslip will result in further decreases in vertical-tail load per unit restoring moment. Fortunately, the addition of the strakes accomplishes both of these desirable effects at high angles of attack, that is, it results in a positive $\left(C_{n_\beta}\right)_{wf}$ and a decrease in $\left(C_{N_\beta}\right)_V$ It therefore appears that addition of the strakes will result in an appreciable reduction in the vertical-tail load per unit yawing moment. This is illustrated in figure 12 where the vertical-tail normal force per unit restoring moment $\frac{C_{N,V}}{C_n}$ is plotted as a function of angle of attack for the complete configuration both with and without the fuselage strakes. Without the fuselage strakes, the vertical-tail normal force increases rapidly above an angle of attack of about 15°. At an angle of attack of 22° a maximum value, of approximately three times the low angle-of-attack value, was reached and above this angle a rapid decrease occurred. With the forebody strakes installed, only a slight increase in tail load occurs and the maximum load encountered with the strakes is only 40 percent of that encountered without the strakes.

CONCLUDING REMARKS

An investigation at high subsonic speeds of the static longitudinal and lateral stability characteristics of a complete model having a delta wing indicated that the addition of fuselage forebody strakes improved the directional stability characteristics at high angles of attack. The results indicated that, despite the inherent tendency for strakes to produce a pitch-up, acceptable pitching-moment characteristics can be obtained provided the strakes are properly chosen and used in conjunction with a wing-body-tail configuration characterized by increasing stability with increasing lift. With regard to directional stability, the addition of the strakes resulted in a reduction in the wing-fuselage instability at moderate angles of attack and resulted in positive directional stability at high angles of attack. This improvement was also reflected in the characteristics of the complete configuration such that the directional stability at high angles of attack was considerably improved. In addition, the loads carried by the exposed vertical tail were measured and it was found that the addition of the strakes, through their favorable effect on the wing-fuselage directional stability, resulted in a considerable reduction in the vertical-tail normal force per unit restoring moment.

Langley Aeronautical Laboratory,
National Advisory Committee for Aeronautics,
Langley Field, Va., October 28, 1957.

REFERENCES

1. Stone, Ralph W., Jr., and Klinar, Walter J.: The Influence of Very Heavy Fuselage Mass Loadings and Long Nose Lengths Upon Oscillations in the Spin. NACA TN 1510, 1948.

2. Phillips, William H.: Effect of Steady Rolling on Longitudinal and Directional Stability. NACA TN 1627, 1948.

3. NACA High-Speed Flight Station: Flight Experience With Two High-Speed Airplanes Having Violent Lateral-Longitudinal Coupling in Aileron Rolls. NACA RM H55A13, 1955.

4. Polhamus, Edward C., and Hallissy, Joseph M., Jr.: Effect of Airplane Configuration on Static Stability at Subsonic and Transonic Speeds. NACA RM L56A09a, 1956.

5. Polhamus, Edward C., and Spreemann, Kenneth P.: Subsonic Wind-Tunnel Investigation of the Effect of Fuselage Afterbody on Directional Stability of Wing-Fuselage Combinations at High Angles of Attack. NACA TN 3896, 1956.

6. Fournier, Paul G.: Low-Speed Investigation of Static Longitudinal and Lateral Stability Characteristics of an Airplane Configuration With a Highly Tapered Wing and With Several Body and Tail Arrangements. NASA TN D-217, 1960. (Supersedes NACA RM L57A08.)

7. Sleeman, William C., Jr.: Investigation at High Subsonic Speeds of the Effects of Various Horizontal Fuselage Forebody Fins on the Directional and Longitudinal Stability of a Complete Model Having a 45° Sweptback Wing. NACA RM L56J25, 1957.

8. Few, Albert G., Jr.: Investigation at High Subsonic Speeds of the Static Longitudinal Stability Characteristics of a Model Having Cropped-Delta and Unswept Wing Plan Forms and Several Tail Configurations. NACA RM L55I23a, 1955.

9. Gillis, Clarence L., Polhamus, Edward C., and Gray, Joseph L., Jr.: Charts for Determining Jet-Boundary Corrections for Complete Models in 7- by 10-Foot Closed Rectangular Wind Tunnels. NACA WR L-123, 1945. (Formerly NACA ARR L5G31.)

10. Herriot, John G.: Blockage Corrections for Three-Dimensional-Flow Closed-Throat Wind Tunnels, With Consideration of the Effect of Compressibility. NACA Rep. 995, 1950. (Supersedes NACA RM A7B28.)

11. Stone, Ralph W., Jr., and Polhamus, Edward C.: Some Effects of Shed Vortices on the Flow Fields Around Stabilizing Tail Surfaces. Rep. 108, AGARD, North Atlantic Treaty Organization (Paris), Apr.-May, 1957.

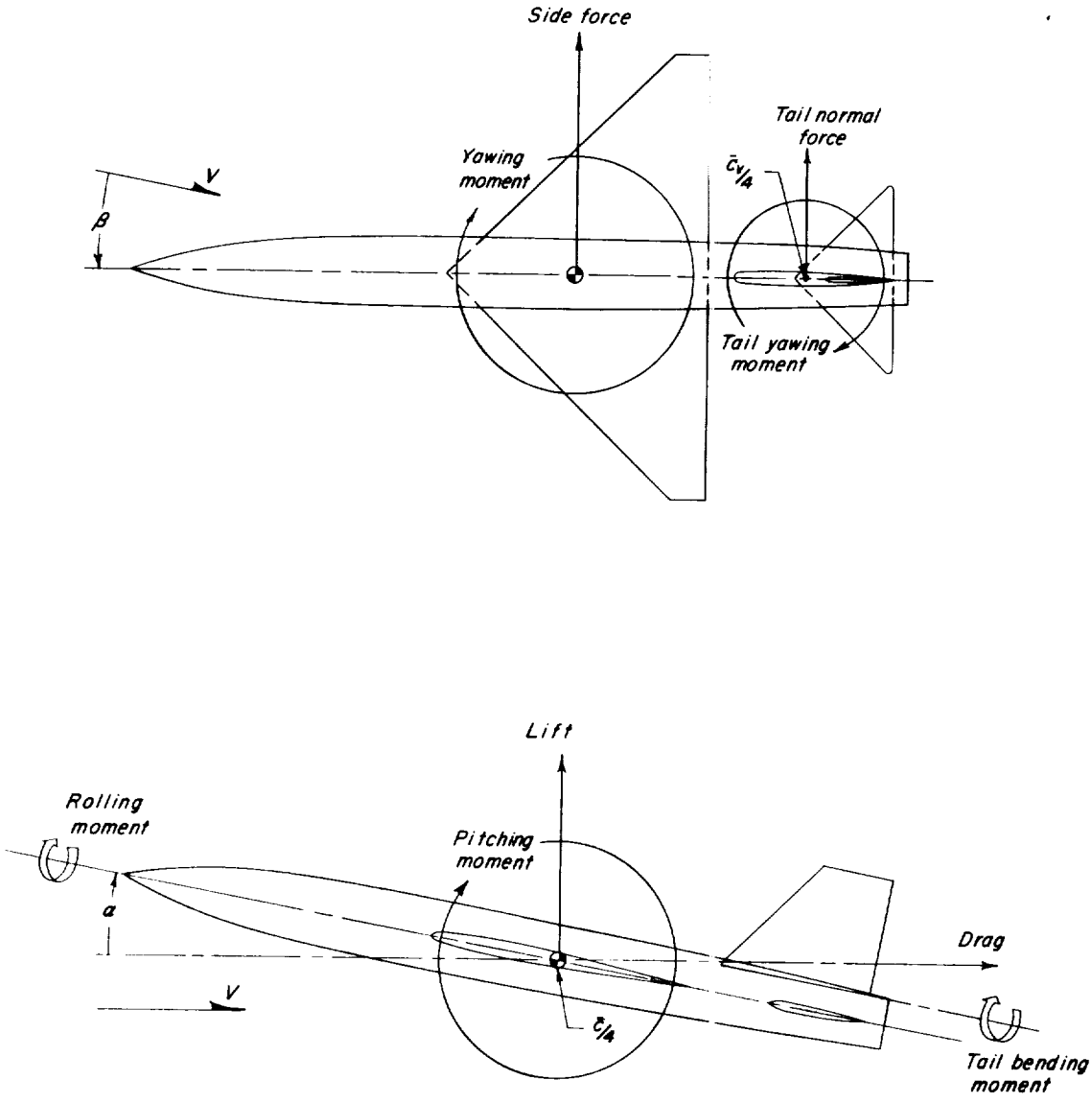

Figure 1.- Reference axes showing positive directions of forces, moments, and angular deflections.

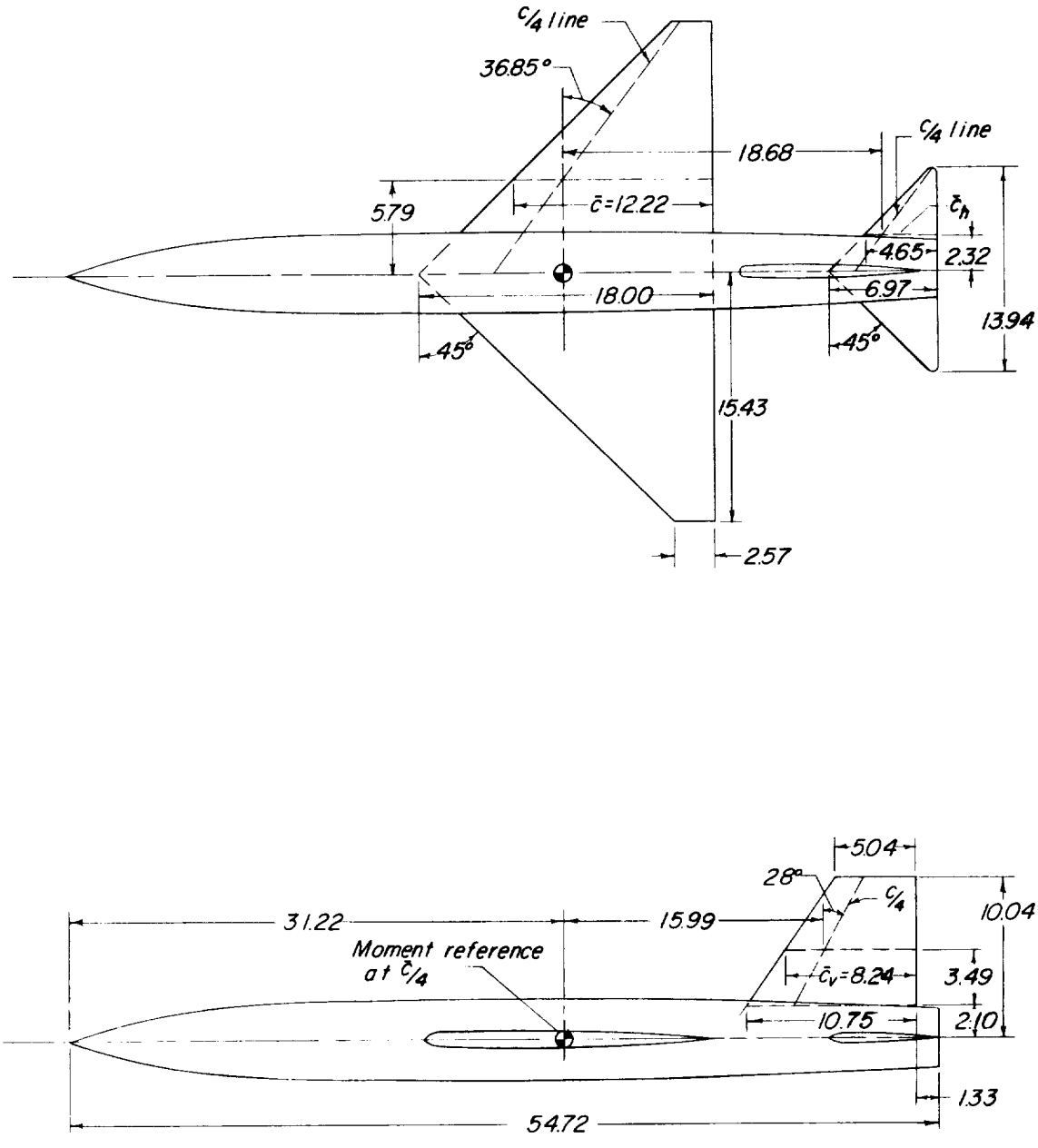

Figure 2.- General arrangement of the basic configuration. Linear dimensions are in inches.

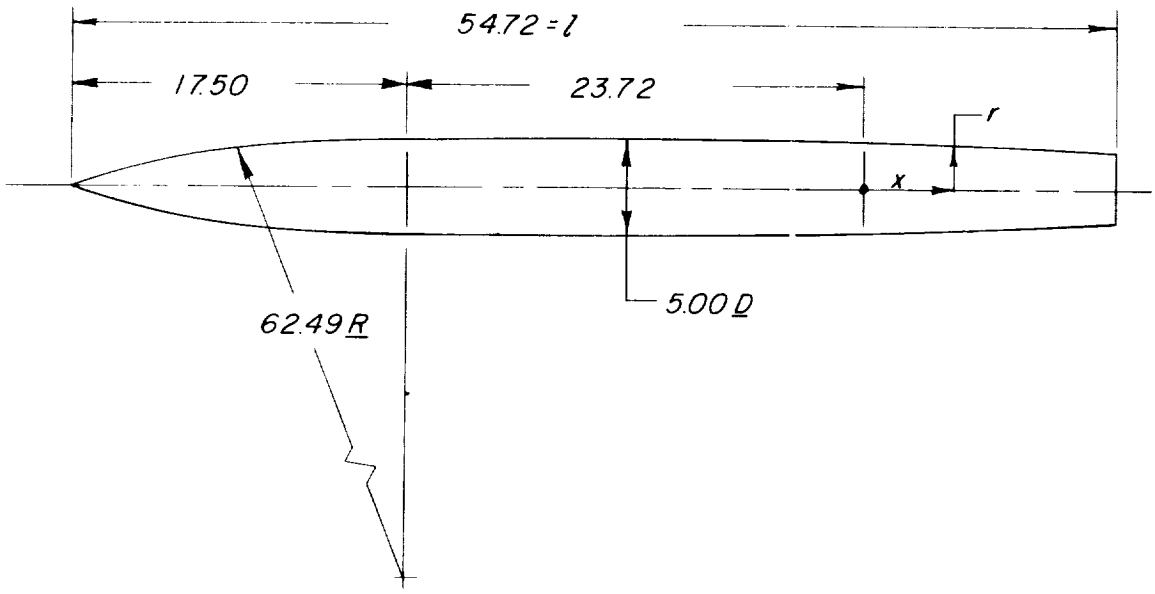

Afterbody Coordinates

x/l	r/l
0	.0456
.0320	.0445
.0639	.0427
.1187	.0390
Straight-line Taper	
.2460	.0301

Figure 3.- Details of the fuselage.

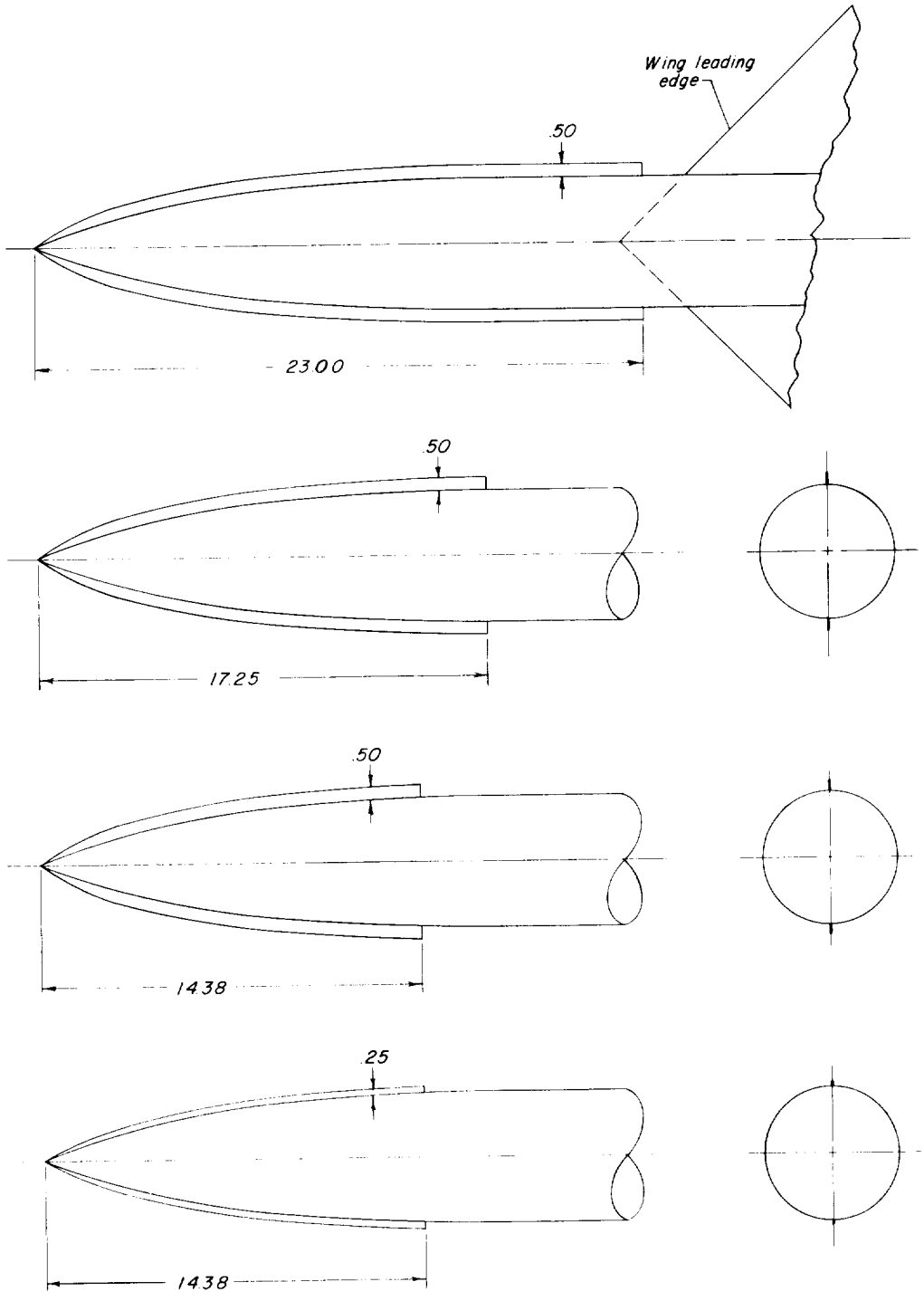

Figure 4.- Details of the various fuselage forebody strakes tested. Dimensions are in inches.

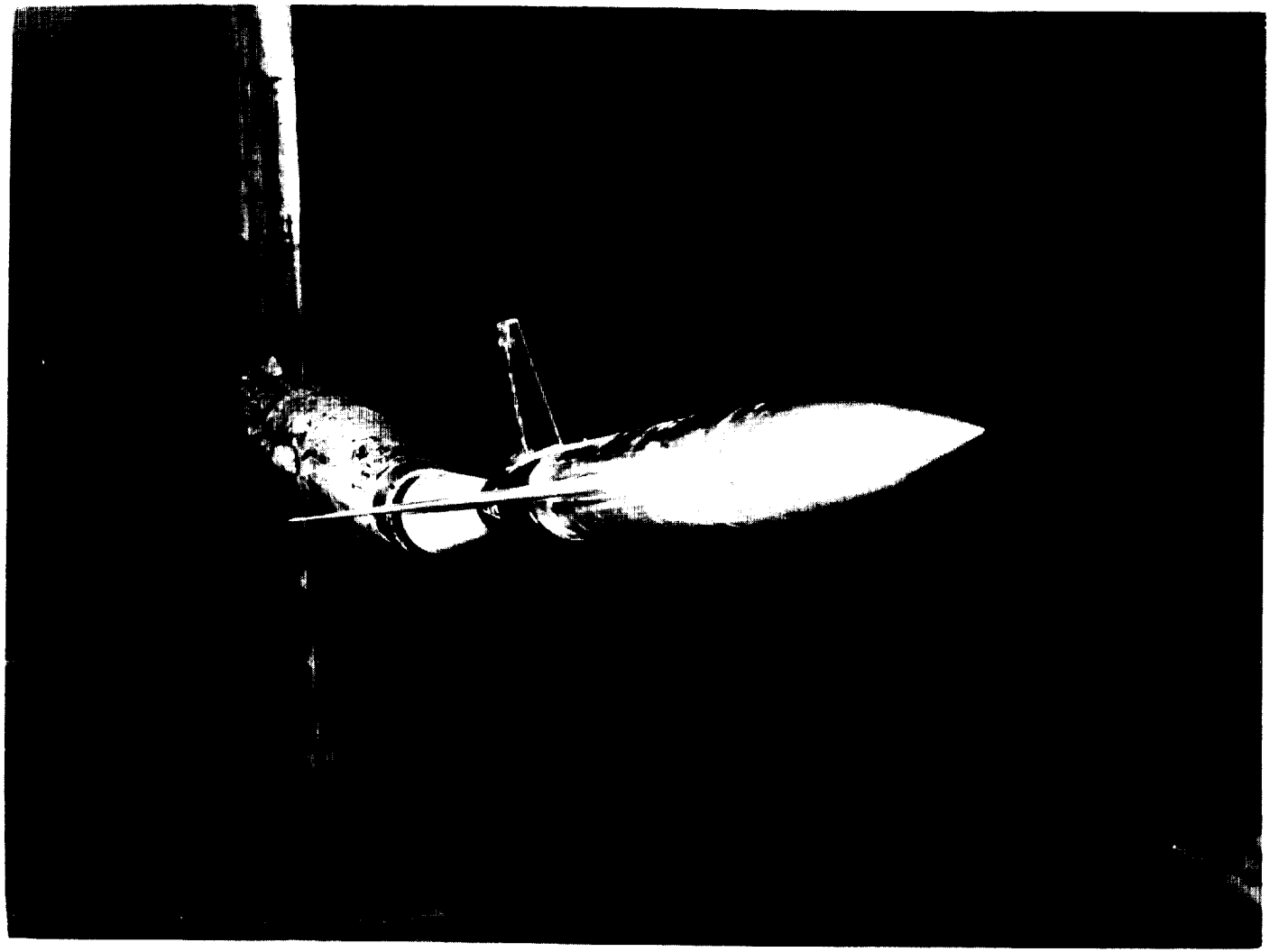

L-83149

Figure 5.- Photograph of the model mounted on the tunnel sting support.

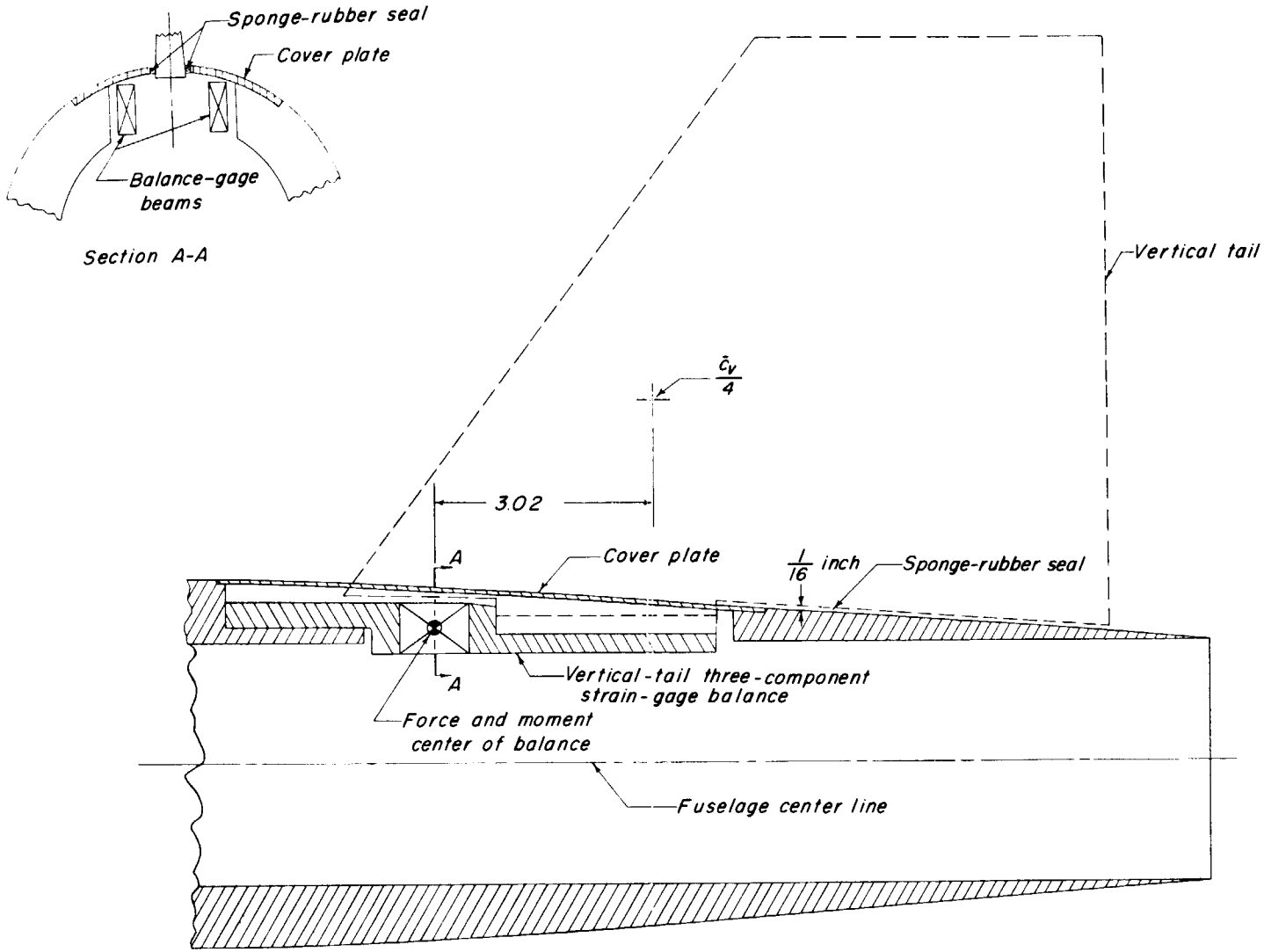

Figure 6.- Drawing of the vertical-tail balance system.

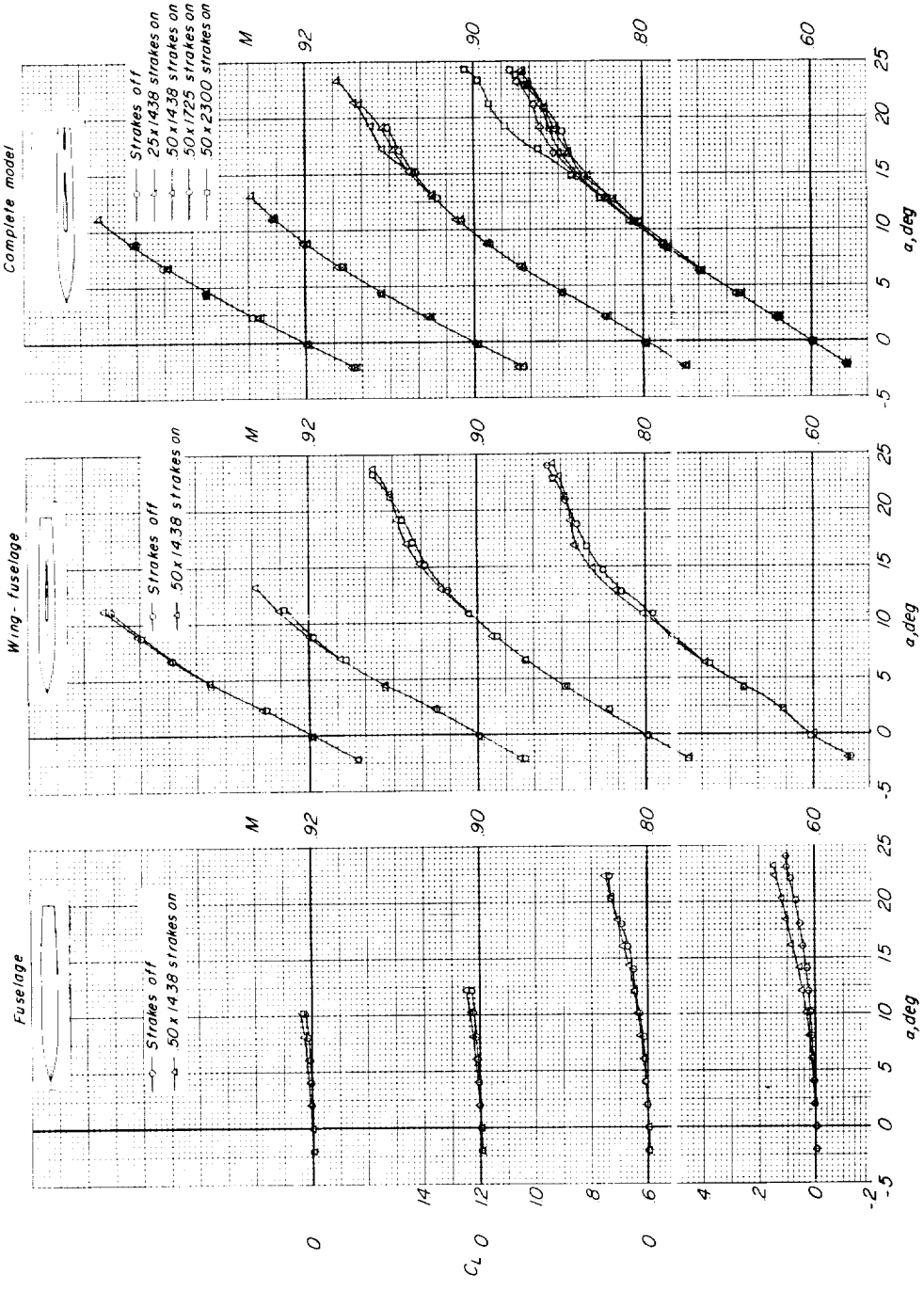

(a) C_L plotted against α.

Figure 7.- Effect of strakes on lift and pitching moment.

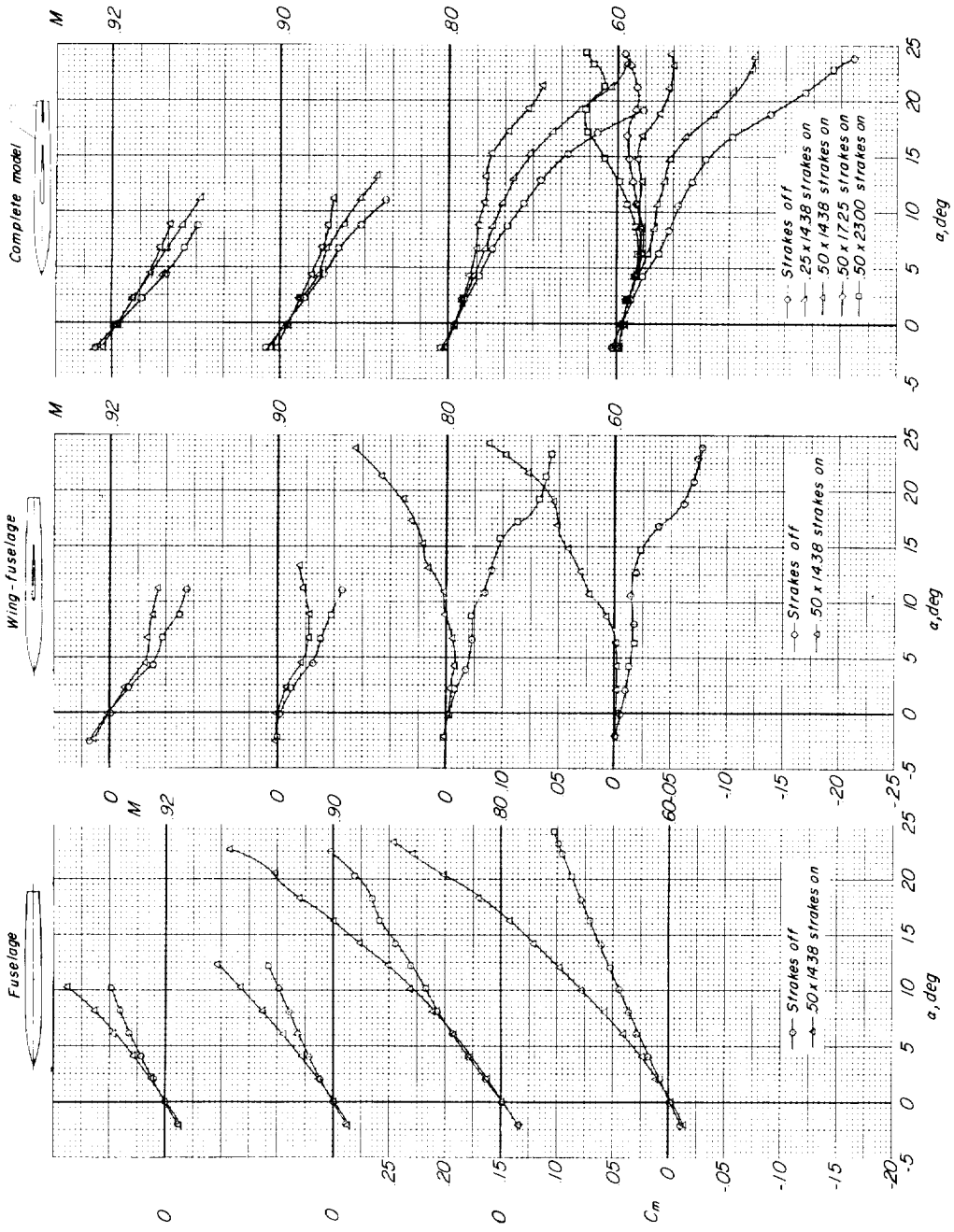

(b) C_m plotted against α.

Figure 7.- Continued.

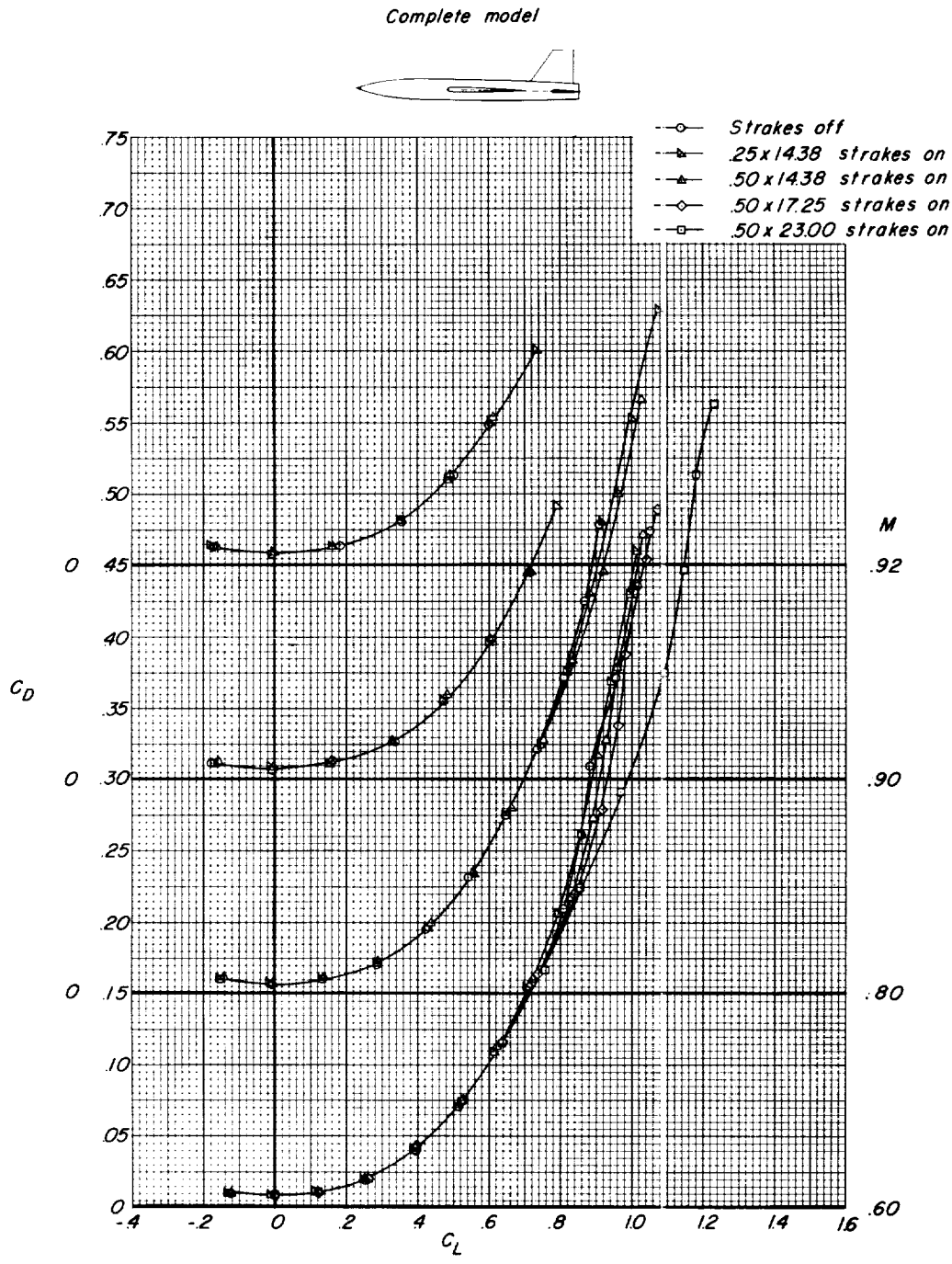

(c) C_D plotted against C_L.

Figure 7.- Concluded.

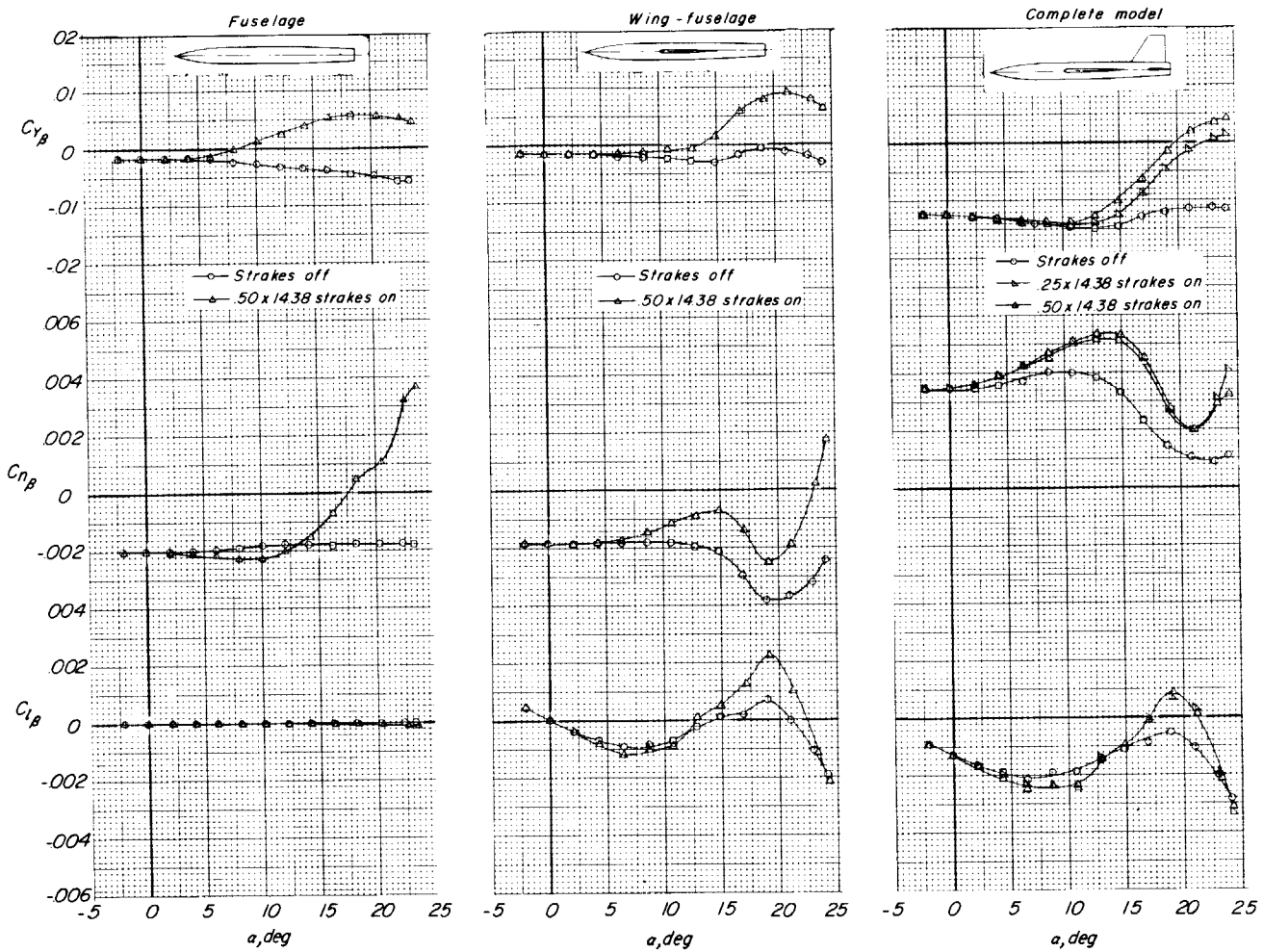

(a) M = 0.60.

Figure 8.- Effect of strakes on the lateral stability parameters.

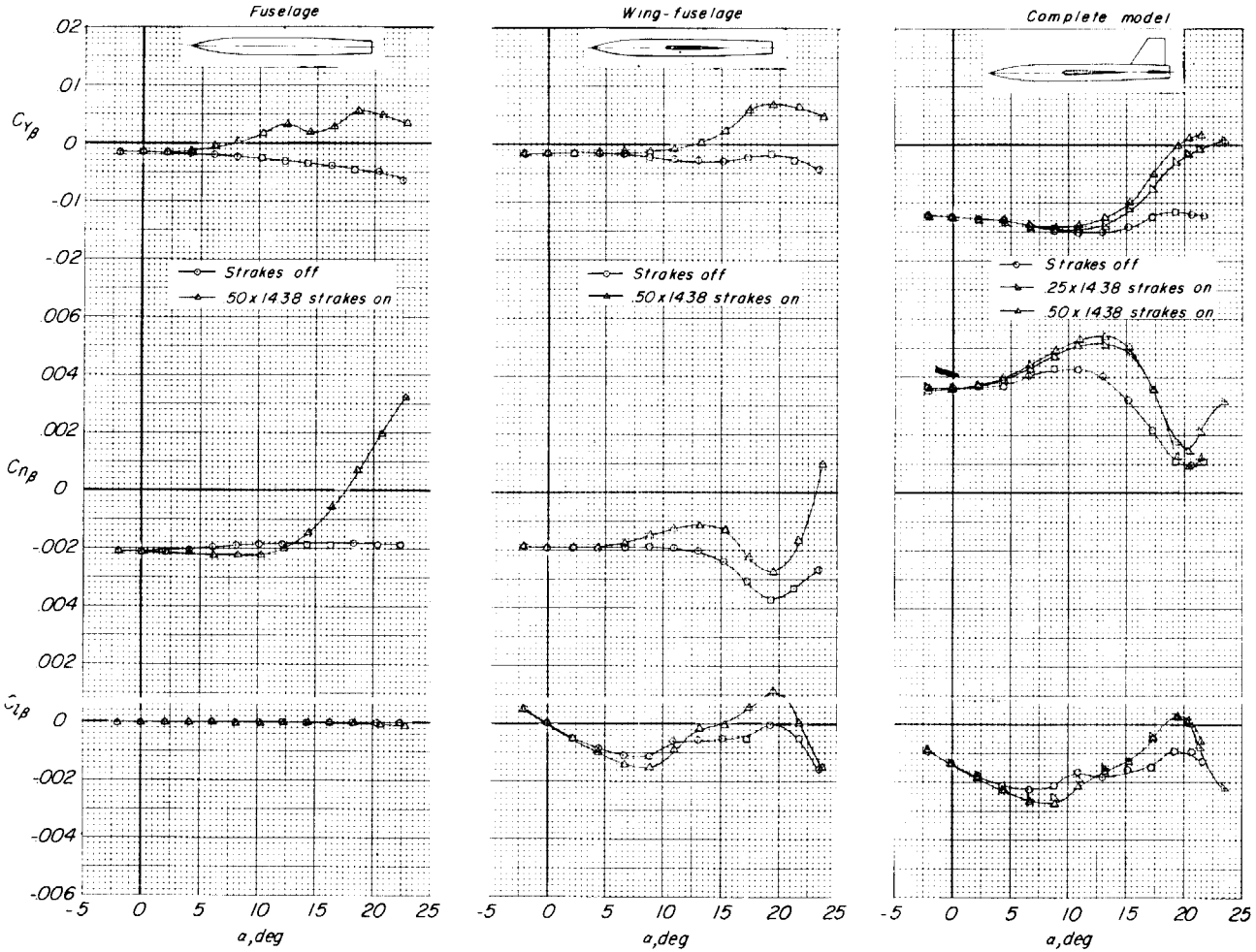

(b) M = 0.80.

Figure 8.- Continued.

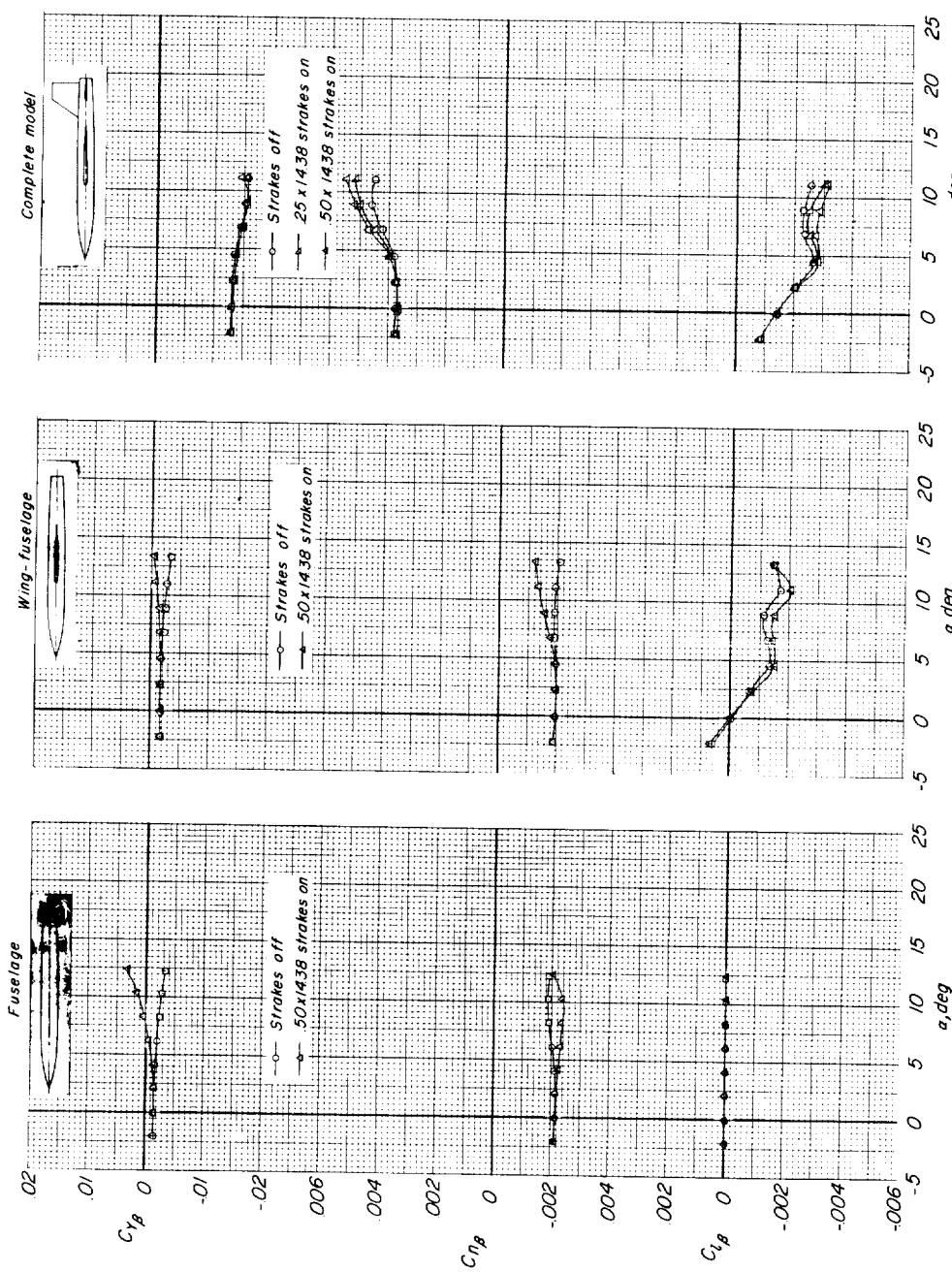

(c) M = 0.90.

Figure 8.- Continued.

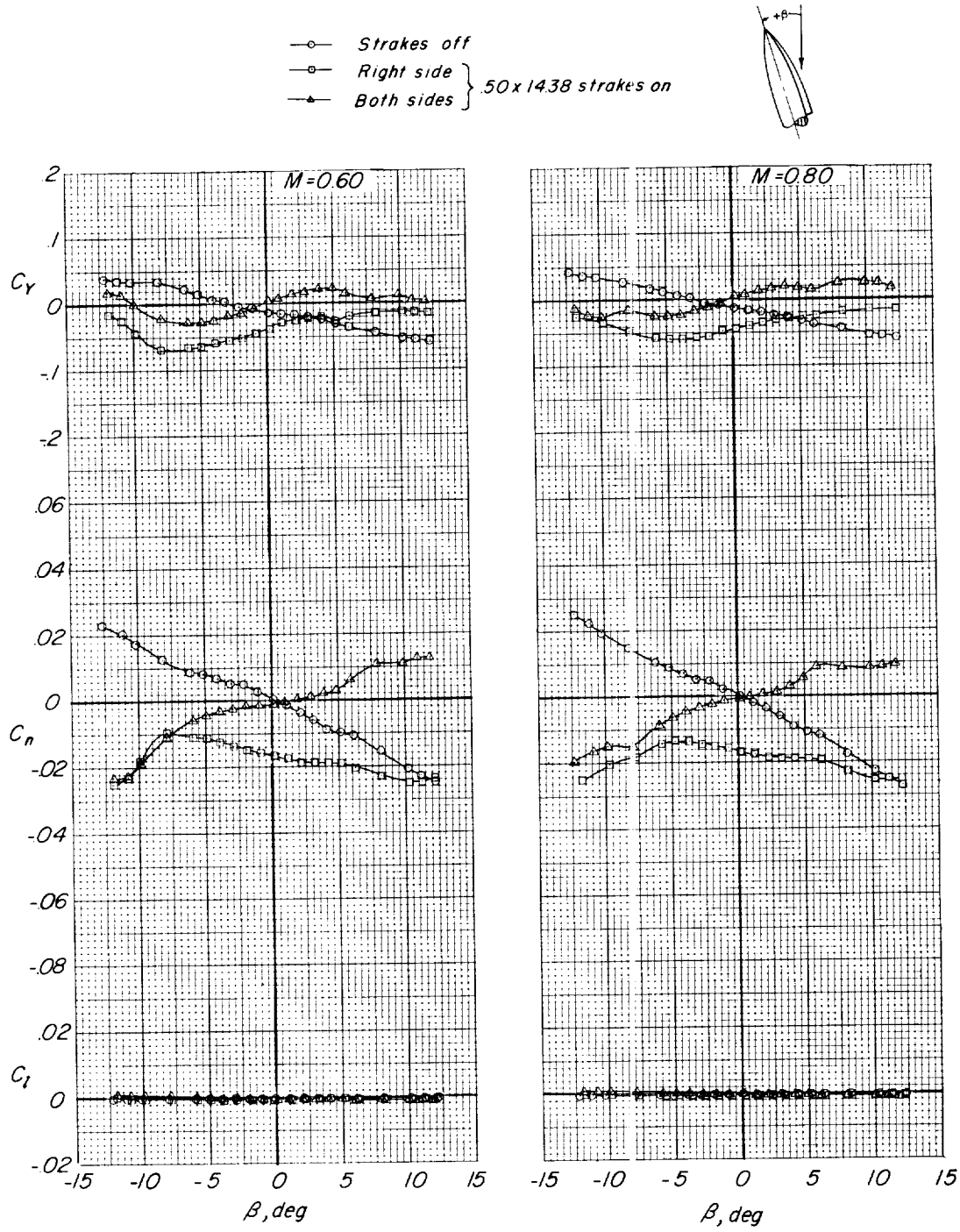

(a) M = 0.60 and M = 0.80.

Figure 10.- Comparison of single and double strakes with regard to sideslip characteristics. $\alpha = 18^{\circ}$; fuselage alone.

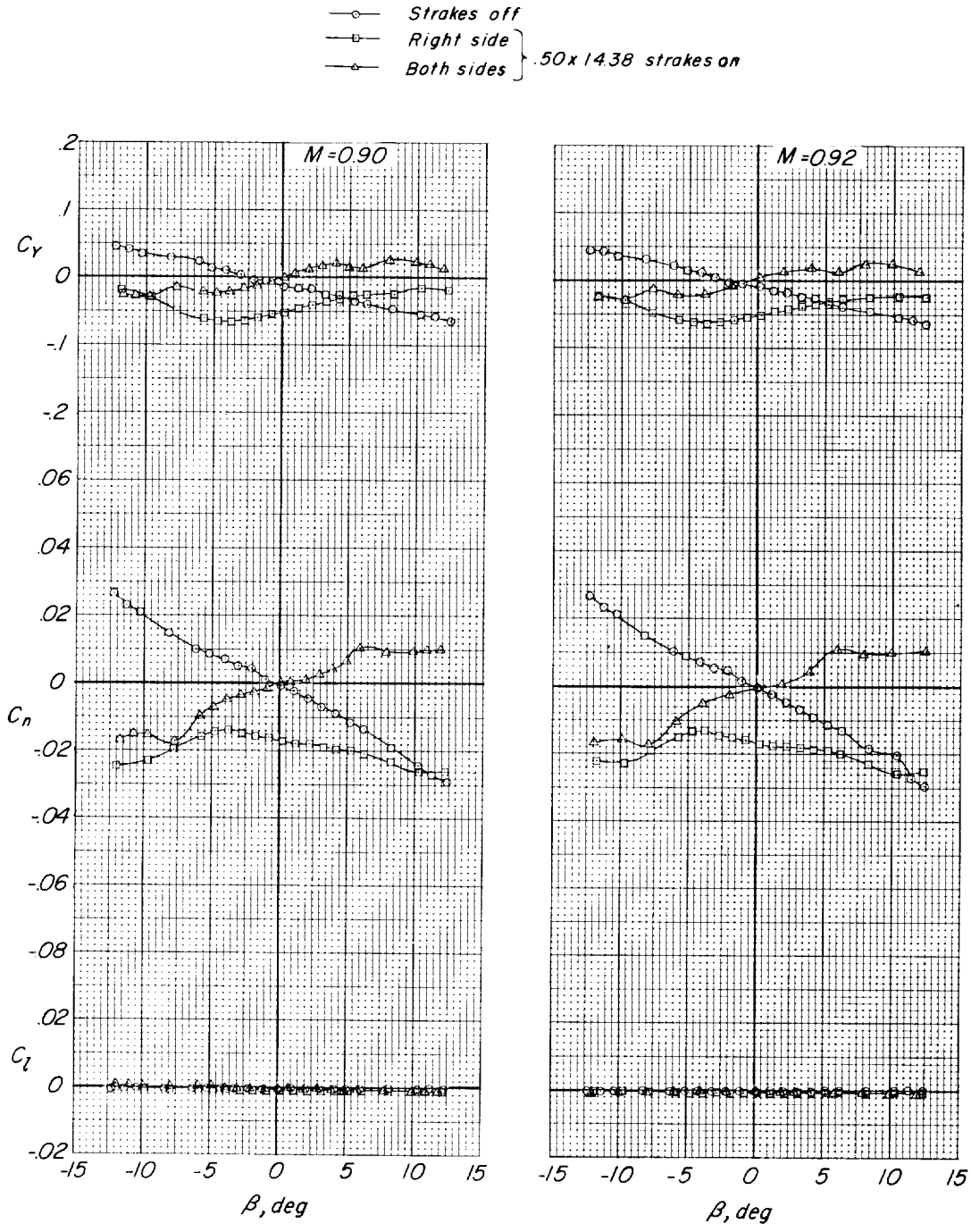

(b) M = 0.90 and M = 0.92.

Figure 10.- Continued.

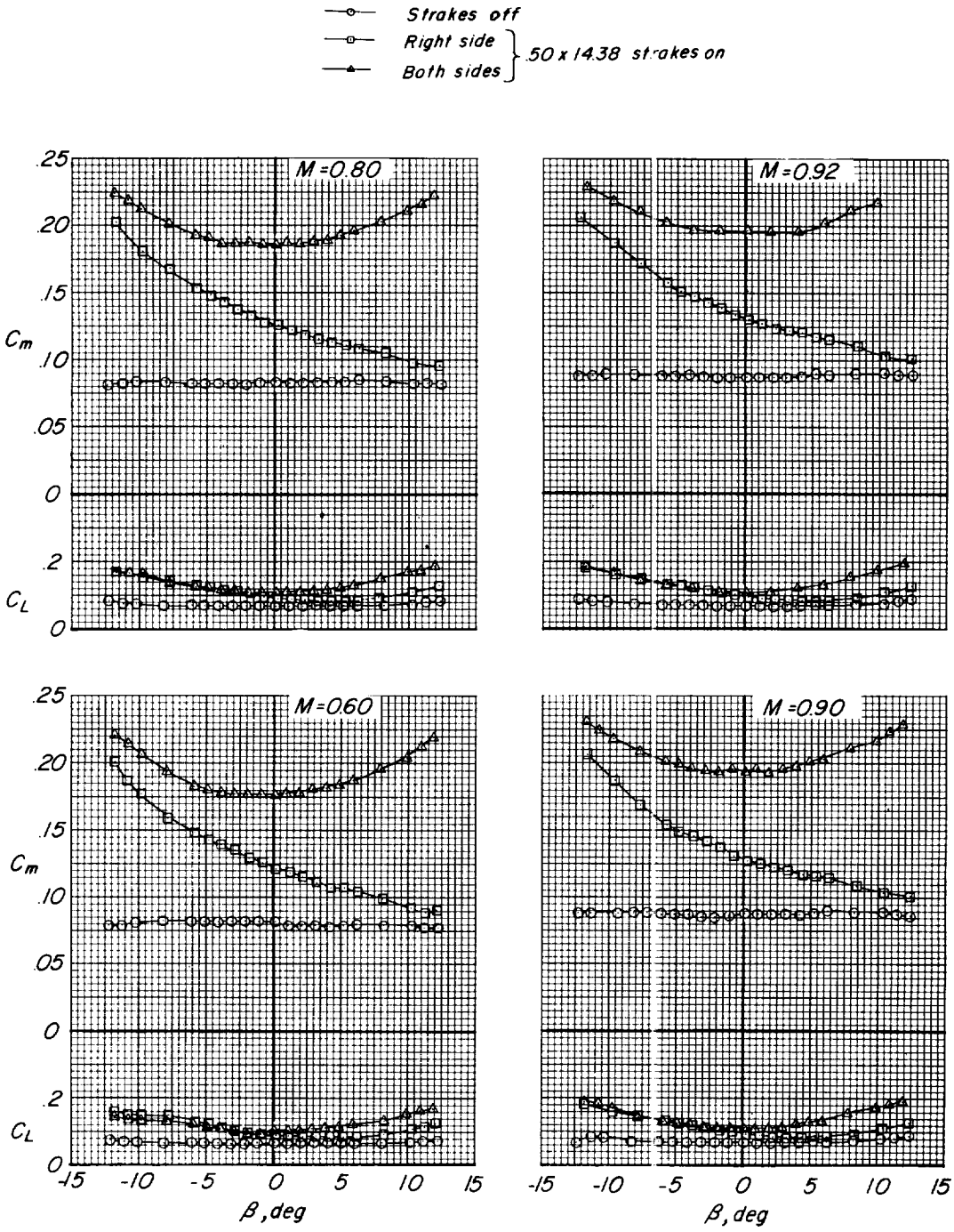

(c) C_m and C_L plotted against β.

Figure 10.- Concluded.

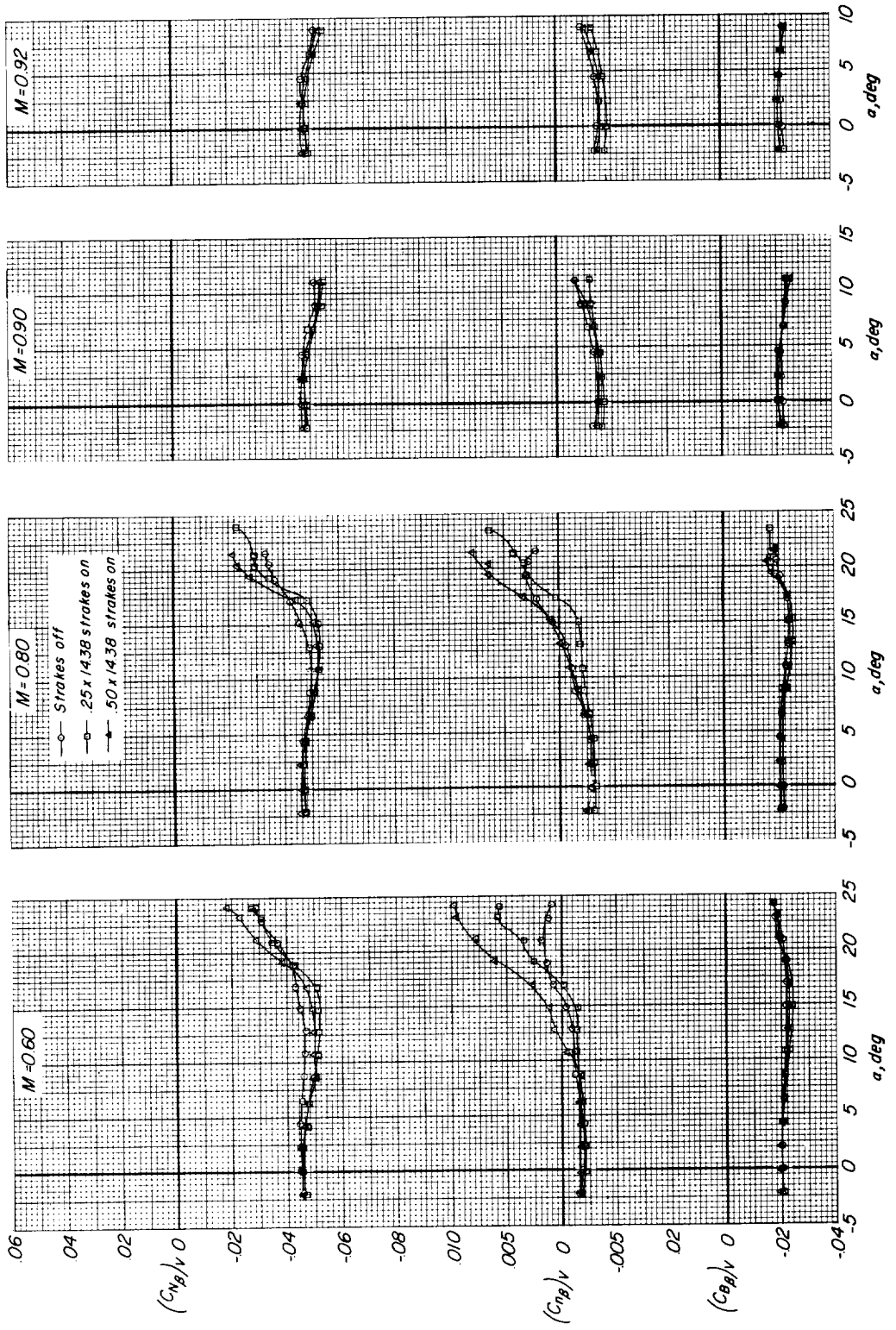

Figure 11.- Effect of strakes on vertical-tail loads.

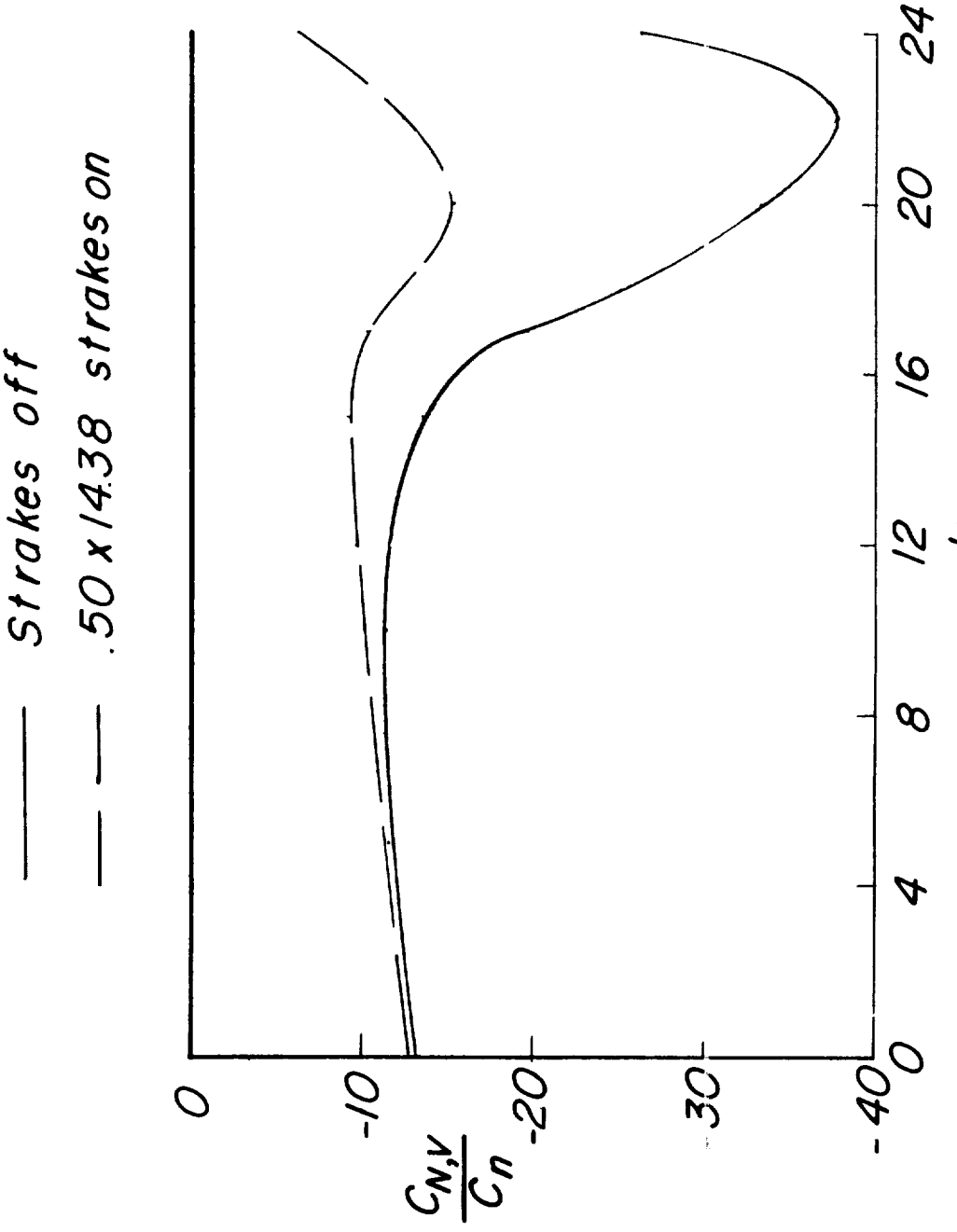

Figure 12.- Effect of strakes on vertical-tail load per unit restoring moment. M = 0.60.